

Activation of the plasma membrane Na/H antiporter Salt-Overly-Sensitive 1 (SOS1) by phosphorylation of an auto-inhibitory C-terminal domain

Francisco J. Quintero^a, Juliana Martinez-Atienza^a, Irene Villalta^a, Xingyu Jiang^a, Woe-Yeon Kim^b, Zhair Ali^b, Hiroaki Fujii^c, Imelda Mendoza^a, Dae-Jin Yun^b, Jian-Kang Zhu^{c,d,1}, and Jose M. Pardo^{a,c,1}

^aInstituto de Recursos Naturales y Agrobiología, Consejo Superior de Investigaciones Científicas, 41012 Sevilla, Spain; ^bDivision of Applied Life Science (BK21 Program), Plant Molecular Biology and Biotechnology Research Center, Graduate School of Gyeongsang National University, Jinju 660-701, South Korea; ^cCenter for Plant Stress Genomics and Technology, King Abdullah University of Science and Technology, Thuwal 23955-6900, Kingdom of Saudi Arabia; ^dDepartment of Horticulture and Landscape Architecture, Purdue University, West Lafayette, IN 47907

Contributed by Jian-Kang Zhu, December 19, 2010 (sent for review November 16, 2010)

The plasma membrane sodium/proton exchanger Salt-Overly-Sensitive 1 (SOS1) is a critical salt tolerance determinant in plants. The SOS2-SOS3 calcium-dependent protein kinase complex up-regulates SOS1 activity, but the mechanistic details of this crucial event remain unresolved. Here we show that SOS1 is maintained in a resting state by a C-terminal auto-inhibitory domain that is the target of SOS2-SOS3. The auto-inhibitory domain interacts intramolecularly with an adjacent domain of SOS1 that is essential for activity. SOS1 is relieved from auto-inhibition upon phosphorylation of the auto-inhibitory domain by SOS2-SOS3. Mutation of the SOS2 phosphorylation and recognition site impeded the activation of SOS1 *in vivo* and *in vitro*. Additional amino acid residues critically important for SOS1 activity and regulation were identified in a genetic screen for hypermorphic alleles.

ion transport | salinity | sodium tolerance

Salinity is a major problem in agriculture because the total area of salt-affected soils, including saline and sodic soils, exceeds 900 million ha (1). Salt-affected soils reduce both the ability of crops to take up water and the availability of mineral nutrients. Often, the high sodium (Na) content relative to other cations is the main factor affecting plant growth by causing a set of metabolic derangements (2). Because most crop species have only very limited capacities to cope with excess Na, the elucidation of Na tolerance mechanisms in plants is of paramount importance (2). Plant ion transporters mediating Na fluxes have recently been cloned and characterized, and the knowledge of the regulatory mechanisms of transporter abundance and activity in response to environmental, hormonal, and developmental signals is critical for understanding salinity tolerance (3).

The plasma membrane Na/H antiporter SOS1 is essential for the salt tolerance of various model plants, including *Arabidopsis thaliana* (4) and its halophytic relative *Thellungiella salsuginea* (5), tomato (6), and the moss *Physcomitrella patens* (7). SOS1 is thought to mediate Na efflux at the root epidermis and long-distance transport from roots to shoots (4, 6) while protecting individual cells from Na toxicity (7–9). SOS1 is also indirectly required for the uptake of potassium (K) in the presence of Na, although the mechanistic basis is not fully understood (7, 8, 10). Both the protein kinase SOS2 and its associated calcium-sensor subunit SOS3 are required for the posttranslational activation of SOS1 Na/H exchange activity in *Arabidopsis* (11, 12), and a similar regulatory module operates also in cereals (13).

To understand further the mechanism(s) of SOS1 regulation, we identified the SOS2-dependent phosphorylation site and began to dissect the structure–function relationship in the SOS1 protein. Our results indicate that the SOS1 C-terminal domain comprises an auto-inhibitory domain the activity of which is counteracted by SOS2-dependent phosphorylation upon salinity stress.

Results

SOS1 Residues Phosphorylated by the SOS2 Protein Kinase. We have previously shown that the plasma membrane Na/H antiporter SOS1 of *Arabidopsis* is regulated positively by the protein kinase complex comprising SOS2 and SOS3 (11, 12). To demonstrate that SOS1 becomes phosphorylated in planta upon salinity stress, the relative mobility of HA-tagged SOS1 was determined in Columbia (Col-0) plants treated or not with 100 mM NaCl. Salt treatment elicited a mobility shift of SOS1-HA (Fig. 1A) that was reversed by incubating the samples with either λ -phosphatase or alkaline phosphatase (Fig. 1B). The phosphorylation-dependent in-gel retardation of SOS1 appeared small due to the large size of the protein (127 kDa). To test whether the phosphorylation of SOS1 was SOS2-dependent, the relative mobility of SOS1 in SDS/PAGE was also analyzed in the *sos2-2* mutant. Because polyclonal antibodies against SOS1 were used in this experiment for protein detection, the *sos1-1* mutant and wild-type plants over-expressing SOS1 were included as controls. The *sos1-1* allele contains a 14-bp deletion causing a frameshift that truncates the SOS1 protein (~49 kDa vs. 127 kDa) (14). The truncated protein does not cross-react with the SOS1 antibodies generated against the C terminus of the SOS1 protein. As shown in Fig. 1C, no in-gel retardation of the SOS1 band was observed in the *sos2-2* mutant compared with that in the wild-type plants. Together these data strongly indicate that SOS2 phosphorylates SOS1 *in vivo* in response to salinity stress.

Next, the amino acid residue(s) of the SOS1 polypeptide that are phosphorylated by SOS2 were determined. There are three distinct modules in SOS1 on the basis of sequence comparisons with other proteins, hydrophobicity, and predicted globular domains by GLOBPLOT (Fig. 2A). The N-terminal module comprises the hydrophobic transmembrane domain encompassing amino acid residues 1–440 that shows sequence homology to other ion exchangers of the CPA1 family from plants and that is likely to act as the pore domain for ion transport (15). Next is an ~300 amino-acid-long stretch that is predicted to comprise a separate globular domain and that, together with the pore domain, presents extensive homology to AtNHX8, a member of the CPA1 family that functions in lithium tolerance in *Arabidopsis* (16). From amino acid 740 to 1146, the SOS1 sequence is unique and does not show significant homology to any other protein except other SOS1-like proteins in plants. The second and third modules (amino acids 441–1146) are predicted to be

Author contributions: F.J.Q., W.-Y.K., D.-J.Y., J.-K.Z., and J.M.P. designed research; F.J.Q., J.M.-A., I.V., X.J., W.-Y.K., Z.A., H.F., and I.M. performed research; and F.J.Q., J.-K.Z., and J.M.P. wrote the paper.

The authors declare no conflict of interest.

¹To whom correspondence may be addressed. E-mail: jkzhu@purdue.edu or pardo@irnase.csic.es.

This article contains supporting information online at www.pnas.org/lookup/suppl/doi:10.1073/pnas.1018921108/-DCSupplemental.

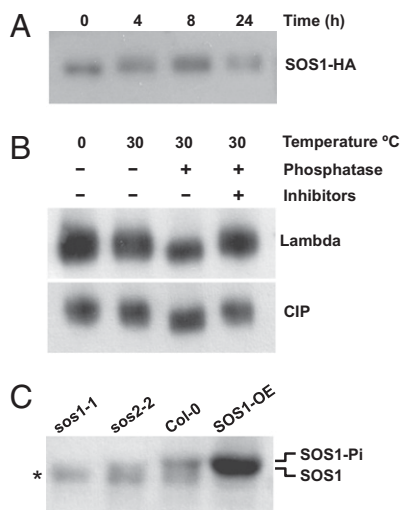


Fig. 1. Phosphorylation of SOS1 in planta. (A) Gel mobility shift of SOS1 elicited by salt treatment. *Arabidopsis* plants were treated with 100 mM NaCl for the time indicated in hours; the protein extracts were resolved by SDS/PAGE, and the HA-tagged SOS1 protein was detected with anti-HA antibodies. (B) Reversal of gel mobility shift by phosphatase treatment. Protein extracts from plants treated with NaCl for 24 h were kept on ice or treated at 30 °C with λ -phosphatase or calf intestinal (CIP) phosphatase with and without the addition of the phosphatase inhibitors; HA-tagged SOS1 protein was detected with anti-HA antibodies. (C) SOS2-dependent mobility shift of SOS1. Protein extracts from mutants *sos1-1*, *sos2-2*, wild-type Col-0 *g1* plants, and the latter transformed to over-express the SOS1 protein were resolved by SDS/PAGE and the SOS1 protein was immunodetected with anti-SOS1 antibodies; plants were treated with 100 mM NaCl for 24 h. The identity of the lower band cross-reacting in all samples (asterisk), including the deletion mutant *sos1-1*, is unknown.

cytosolic. Therefore, nested deletions of the SOS1 hydrophilic tail spanning residues 441 to 1146 were fused to the C-terminal end of GST, affinity purified with GST-Sepharose, and subjected to SOS2-dependent phosphorylation assays (Fig. 2B). The SOS2

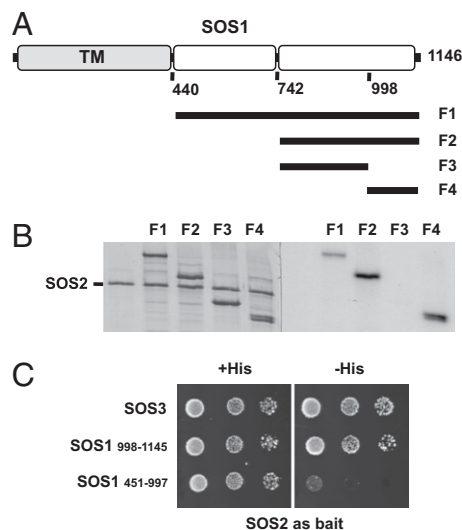


Fig. 2. Phosphorylation of the SOS1 C terminus. (A) Schematic structure and deletion mapping of SOS1; fragments F1–F4 were subjected to the SOS2 phosphorylation assay (B). Purified proteins corresponding to fragments F1–F4 were incubated with SOS2T168D/ Δ 308 in the presence of [γ - 32 P]ATP, resolved in SDS/PAGE (Left), and exposed to X-ray film (Right). (C) Yeast two-hybrid assay demonstrating the interaction of SOS2 with the last 147 amino acids of SOS1.

derivative SOS2T168D/ Δ 308 was used because this mutant protein has much higher protein kinase activity than wild-type SOS2 and is independent of SOS3 (17). The SOS1 peptide comprising amino acids 1072–1146 was the smallest fragment phosphorylated by SOS2, indicating that SOS2 phosphorylates SOS1 at the very end of this large protein. In keeping with this, full-length SOS2 interacted with the SOS1998–1145 fragment, but not with the SOS1451–997 fragment in the yeast two-hybrid system (Fig. 2C).

To identify the actual phosphorylated residues, fragment SOS1998–1146 was incubated with the SOS2T168D/ Δ 308 kinase in the presence of ATP and then subjected to nano-liquid chromatography tandem mass-spectrometry analysis (nLC-MS/MS). An untreated SOS1998–1146 sample was used as control to discard phosphorylation events that may have taken place in the yeast cells before protein purification. The phosphopeptide of sequence IDSPpSKIVFR, corresponding to amino acids 1134–1143 and in which the serine in position 1138 appeared phosphorylated, was specifically identified by nLC-MS/MS in the SOS1 sample incubated with SOS2T168D/ Δ 308 but not in the control sample. Prior biochemical characterization of SOS2 indicated a phosphorylation recognition site similar to those of SNF1/AMPK/SnRK protein kinases with the consensus H-X-B-X₂-(S/T)-X₃-H, where “H” indicates hydrophobic residues, “B” is a basic residue, and “S/T” is the phosphorylation site (18). Thus, S1136, which is embedded in the sequence IVVRIDSPSKIV (serines 1136 and 1138 are underlined), is a better match with the consensus than S1138. To validate nLC-MS/MS results and to check whether S1136 could be also involved in the phosphorylation of SOS1, serine-to-alanine mutations were introduced in positions S1136 and S1138 either individually or in combination. The entire cytosolic region of SOS1 (amino acids 441–1146), with and without S1136A/S1138A mutations, was tested in SOS2-dependent phosphorylation assays. Both mutations S1136A and S1138A prevented phosphorylation by SOS2 (Fig. 3A). Thus, it appears that S1138 is phosphorylated by SOS2, whereas S1136 is essential for substrate recognition by the protein kinase. No other residues of SOS1 appeared to be phosphorylated by SOS2 in the

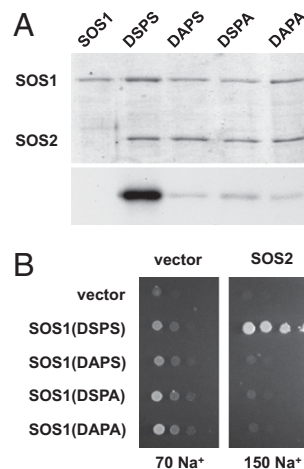


Fig. 3. Serines 1136 and 1138 in the SOS2 phosphorylation site are essential for SOS1 activation. (A) GST fusions encompassing the SOS1 cytosolic tail (amino acids 441–1146) from the wild-type protein (D5PS), mutant S1136A (D4PS), mutant S1138A (D5PA), and mutant S1136A/S1138A (D4PA) were subjected to phosphorylation by SOS2 in vitro, resolved by SDS/PAGE (Upper) and exposed to X-ray film (Lower). (B) Full-length wild-type or mutant SOS1 proteins were expressed in the yeast strain AXT3K with (Right) or without (Left) the coexpression of SOS2T168D/ Δ 308. Decimal dilutions of saturated cultures were plated in AP medium supplemented with 1 mM KCl and with the indicated concentration of NaCl. Growth of all transformants was indistinguishable in plates without NaCl.

SOS1441-1146 fragment as efficiently as S1138. Background phosphorylation in mutant proteins likely occurred at places in the cytosolic region of SOS1 weakly conforming to SNF1/AMPK/SnRK recognition sites. A survey of all SOS1-like sequences in public databases showed that the SOS2 phosphorylation site identified here is conserved in nearly all plant sequences available, with the consensus [V,I]VR[V,I]DPS (Fig. S1C). There are few motifs that depart from this consensus among the SOS1 sequences available in protein databases. The most dissimilar is the tomato SOS1 protein where the DPS motif is interrupted by two intervening amino acids.

Residues S1136 and S1138 Are Essential for the Activation of SOS1 in Vivo. To assess the requirement of the phosphorylation by SOS2 on the activation of SOS1, proteins carrying single or combined S1136A and S1138A mutations were expressed in the salt-sensitive yeast strain AXT3K, with and without coexpression of SOS2T168D/Δ308, and the capacity to grow on media with NaCl was determined. As depicted in Fig. 3B, the mutant proteins conferred the same degree of salt tolerance as the wild-type SOS1 in the absence of SOS2, indicating that the basal activity of the transporter had not been affected by the S1136A and/or S1138A mutations. Wild-type SOS1 coexpressed with SOS2T168D/Δ308 produced a remarkable increase of salt tolerance, allowing the growth of yeast cells in the presence of 200 mM NaCl. By contrast, no increase in salt tolerance was observed when SOS2T168D/Δ308 was coexpressed with either one of the SOS1 proteins harboring mutations S1136A and/or S1138A. As expected, the kinase-dead mutant SOS2K40N/T168D/Δ308 (17) failed to activate wild-type SOS1 or S-to-A mutants in yeast cells, implying that phosphorylation by SOS2 is essential for SOS1 activation. The SOS1 variants with mutations S1136A and/or S1138A were also tested for complementation of the knock-out allele *sos1-1* of Arabidopsis. Five-day-old T2 transgenic seedlings expressing the SOS1S1136A/S1138A mutant allele under the 35S cauliflower mosaic virus (CaMV) promoter were germinated on Murashige-Skoog (MS) medium and then transferred to plates with 50 or 100 mM NaCl for 15 d. The nonphosphorylatable SOS1 mutant protein failed to complement *sos1-1* under 100 mM NaCl treatment. However, growth was partially restored in 50 mM NaCl compared with plants transformed with the empty vector, but these lines did not reach the growth rate produced by wild-type protein (Fig. S2A and B). This partial complementation in low salt is likely due to the basal activity of SOS1, in keeping with the residual growth of yeast cells expressing the mutant SOS1 proteins. Indeed, the salt tolerance of the *sos1-1* transgenic lines expressing SOS1S1136A/S1138A was equivalent to that of the *sos2-2* mutant (Fig. S2C), in which the wild-type SOS1 protein remains in a state with basal activity (11, 12). Similar results were obtained with the single-site mutant protein SOS1S1136A (Fig. S2D). Together, these results demonstrate that phosphorylation at S1138 by SOS2 is an essential step for the activation of SOS1 in response to salt stress. To further demonstrate that SOS2-dependent phosphorylation is also sufficient for the activation of ion transport, a His-tagged SOS1 protein was purified from yeast plasma membrane and reconstituted in artificial proteoliposomes. Efflux of luminal protons by Na/H exchange was monitored by pyranine fluorescence recovery after the addition of 50 mM Na₂SO₄ (Fig. S3A). As depicted in Fig. S3B, the addition of SOS2T168D/Δ308 in the presence of ATP stimulated Na⁺ transport by SOS1.

Auto-Inhibitory Domain in SOS1. To gain further insights into the structure–function relationships of SOS1, a mutant screen for gain-of-function alleles of *SOS1* was performed. Expression of wild-type SOS1 in the yeast strain AXT3K improves growth in medium containing moderate concentrations of NaCl (up to 50 mM NaCl), whereas coexpression of SOS2 and SOS3 allow yeast cells to grow in 200 mM salt concentration (11). Hence, muta-

tions locking SOS1 in the activated state in the absence of SOS2–SOS3 could be selected on medium containing the appropriate NaCl concentration. A randomly mutagenized population (~2 × 10⁵ independent clones) of *SOS1* was created using the *Escherichia coli* hypermutable strain XL1-Red. The mutagenized plasmids were recovered in six independent pools and then transformed into the yeast strain AXT3K. Transformants were selected in arginine-phosphate (AP) medium supplemented with 1 mM KCl and 150 mM NaCl, a salt concentration that completely inhibits the growth of yeast cells expressing wild-type SOS1. Forty-four independent, salt-tolerant clones were isolated that were further classified into two groups according to their relative salt tolerance and their response to SOS2–SOS3 (Table S1). Transformants of class 1 tolerated 200 mM NaCl in the absence of SOS2–SOS3, but salt tolerance increased to 400 mM NaCl when the mutant SOS1 protein was coexpressed with the SOS2–SOS3 protein complex (Fig. 4A). Transformants of class 2 showed extreme resistance to salt and were able to grow up to 800 mM NaCl (in AP medium with 1 mM KCl), but their halotolerance was not further increased by coexpression of SOS2–SOS3. Incremental levels of NaCl tolerance strictly correlated with reduced net uptake of Na⁺ in yeast transformants. A disproportionate amount of individual class 2 clones were isolated relative to class 1 clones. Several clones shared the same mutation even though they were isolated from different pools of mutagenized plasmids, indicating that they were redundant mutations that originated from independent events. In total, 11 different mutations were identified, 6 of them belonging to class 1 and 5 to class 2 mutants (Table S1). Class 1 mutations E281K, A399V, and A399T mapped at the putative 7th and 11th transmembrane

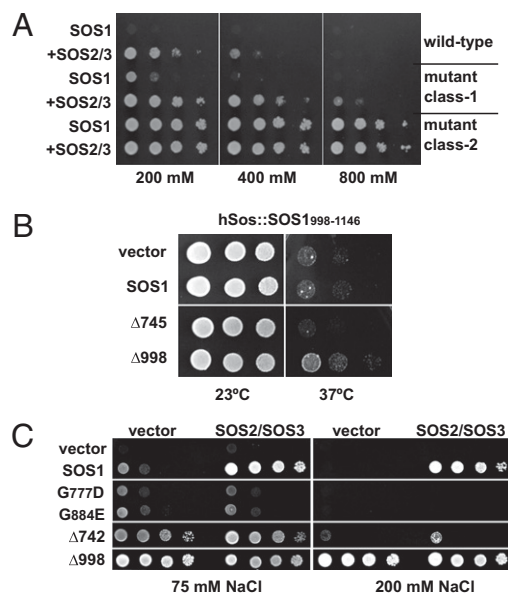


Fig. 4. Functional domains of SOS1. (A) Representative class 1 and class 2 mutants were transformed in strain AXT3K, with and without the coexpression of the SOS2–SOS3 kinase complex, and compared with wild-type SOS1 in AP medium (1 mM KCl) with the indicated concentrations of NaCl. All transformants had identical growth in plates without NaCl. (B) The yeast mutant *cdc25-2*, transformed with the reporter protein hSos::SOS1998-1146, was further transformed to express wild-type SOS1, or mutant proteins truncated at residues 745 and 998, or with an empty vector. Decimal dilutions of liquid cultures were plated and incubated at the permissive (23 °C) or restrictive (37 °C) temperature to identify protein interactions at the plasma membrane. (C) Salt-tolerance test of AXT3K cells expressing the indicated SOS1 mutant proteins with and without the coexpression of the SOS2–SOS3 kinase complex.

segments (TMs). Mutation R551G is in the central part of the cytosolic domain, and mutations S742L and V743I cluster together at the junction between the SOS1 segment that is highly homologous to AtNHX8 and the SOS1-specific C-terminal tail. Interestingly, class 2 mutations were all clustered (residues P985, Q998, Q1000, K1005, and W1013), and all but mutation P985S produced premature stop codons, thereby creating C-terminal deletions.

The finding that class 2 mutants showed maximal SOS1 activity and were impervious to the SOS2–SOS3 kinase complex (Fig. 4A) suggested that the last ~130 residues of the SOS1 protein act as an auto-inhibitory domain. Also, because no other class 2 mutations were isolated farther downstream from the residue W1013 despite the redundancy of isolates with class 2 mutations (Table S1), the putative auto-inhibitory domain was likely downstream from and adjacent to the cluster of class 2 mutations (see diagram in Fig. S4A). To confirm this, stop codons were introduced in residues L1030, N1047, and L1072 by site-directed mutagenesis. Also, the loss-of-function allele *sos1-11* isolated in *Arabidopsis* (14), consisting of a frameshift mutation in residue L1106, was created in the *SOS1* cDNA. Mutant proteins with these nested deletions were expressed in yeast with and without SOS2T168D/Δ308. The relative salt tolerance of these transformants showed that mutant SOS1Δ1030 had a basal activity greater than that of wild-type SOS1 (Fig. S4B) but much lower than that of class 2 mutants (Fig. 4A), suggesting that the auto-inhibitory domain was partly active in this mutant. By contrast, mutants with truncations at N1047, L1072, and L1106 showed low basal activity equivalent to the wild-type protein demonstrating that the auto-inhibitory domain was present and fully functional. Neither of these mutants could be activated by SOS2T168D/Δ308, as expected from the removal of the phosphorylation site by SOS2. Together with the derepressed state of the class 2 mutant SOS1W1013Z, these results indicate that the auto-inhibitory domain spans from amino acid W1013 to N1047. There are two motifs within this stretch that are conserved in SOS1-like proteins and that may comprise the auto-inhibitory domain: [K,R][D,E]HxGLxSWPE (residues K1005 and W1013 mutated in class 2 mutants are underlined) and Sx[R,K]Axx[L,I,V]S[I,M][F,Y]GS (amino acids 1033–1044) (Fig. S1B). The finding that both truncation at W1013 within the first conserved motif and truncation at L1030 in the intervening sequence between the two conserved motifs conveyed lower constitutive salt tolerance than other class 2 mutant proteins strongly indicate that the auto-inhibitory domain was partly active in these truncated proteins and that the two conserved motifs identified here together constitute the auto-inhibitory domain of SOS1.

Auto-Inhibitory Domain Interacts with a Conserved Domain That Is Essential for SOS1 Activity. An activation mechanism of SOS1 consisting of counteracting auto-inhibition predicts that the inhibitory domain interacts with another domain of SOS1 to keep the transporter in a resting state with basal activity. To test this idea, the human Son-of-Sevenless (hSos) recruitment system (SRS) was used to monitor in yeast the in vivo interaction between wild-type and truncated SOS1 proteins residing on the plasma membrane (bait) and a cytosolic reporter protein (prey) consisting of the auto-inhibitory domain SOS1998-1146 fused to the human hSos protein. Upon interaction of prey and bait proteins, recruitment of the hSos to the plasma membrane restored Ras guanyl nucleotide exchange factor activity and growth at 37 °C of the thermosensitive yeast mutant *cdc25-2* (19). The interaction of the reporter protein (hSos: SOS1998-1146) was tested using as bait the full-length SOS1 protein and the SOS1 proteins truncated at position 998 (SOS1Δ998) or 742 (SOS1Δ742), i.e., lacking only the auto-inhibitory domain or the entire module that is specific to SOS1-like proteins, respectively (Fig. 2A). As depicted in Fig. 4B, the reporter protein hSos:SOS1998-1146 was recruited to the plasma membrane upon

coexpression of SOS1Δ998. Interaction of the reporter protein with the wild-type SOS1 is probably hindered because the docking site is already occupied by its own auto-inhibitory domain acting in cis. Interaction was lost with the truncated protein SOS1Δ742 indicating that the target sequence of the auto-inhibitory domain is located between positions 742 and 998. Within this region there is a highly conserved stretch, from residue 764 to 849, that shows homology with cyclic nucleotide-binding domains (CNBDs; Prosite pf00027; Fig. S1A) and that is known to play an essential yet undetermined role in SOS1 function (14). In *Arabidopsis*, loss-of-function alleles *sos1-8* and *sos1-9* consist of single-point mutations that are translated to amino acid changes G777D and G784E, respectively, affecting two fully conserved G residues in this putative CNBD (14). To evaluate the role of this domain in the activity and regulation of SOS1, the cDNAs encoding SOS1Δ742, which had the CNBD removed, and the mutant alleles *sos1-8* and *sos1-9* were expressed in yeast, and the salt tolerance that they conveyed was determined. As shown in Fig. 4C, the absence of the 742–998 region produced a great reduction of salt tolerance compared with the wild-type SOS1 activated by coexpression of SOS2–SOS3 and with the SOS1Δ998 lacking the auto-inhibitory domain. However, the SOS1Δ742 protein demonstrated greater salt tolerance than wild-type SOS1 alone, likely as the result of having the auto-inhibitory domain removed. It is worth noting that this protein would be equivalent to AtNHX8 (16). On the other hand, mutant proteins SOS1G777D (*sos1-8* allele) and SOS1G784E (*sos1-9*) retained a basal activity similar to that of wild-type SOS1, but contrary to the latter they could not be activated by SOS2–SOS3. Accordingly, the SOS1G777D protein (*sos1-8* allele) could not be activated by SOS2 in transport assays (Fig. S3). Deletion of the auto-inhibitory domain in SOS1G777D (*sos1-8*) produced only a marginal increase in salt tolerance, indicating that the mutation G777D is epistatic over the derepressed state of SOS1Δ998 (Fig. S4C).

Discussion

Here we show that phosphorylation by SOS2 is both necessary and sufficient to activate SOS1. Serine 1138 within the highly conserved consensus motif [V,I]VR[V,I]DSPS (serine 1138 underlined) was identified as the SOS2 phosphorylation site. However, serine 1136 fitted better the hypothetical recognition site H-X-B-X2-(S/T)-X3-H (18). Mutations S1136A or S1138A prevented SOS1 phosphorylation by SOS2. Moreover, mutation of S1136 to aspartate, which mimics the negative charge of a phosphorylated residue, yielded an inactive SOS1 protein (Fig. S2D). The simplest explanation for these observations is that S1138 is phosphorylated by SOS2, whereas S1136 is essential for substrate recognition by the protein kinase. However, while this work was being completed, Yu et al. (20) reported that the MAP kinase MPK6 phosphorylated the C-terminal fragment of SOS1, although neither the precise phosphorylated residue nor the effect on SOS1 activity was determined. The motif RIDSPSK of SOS1 also conforms to a proline-directed MAPK site in which S1136 preceding the proline residue would be phosphorylated. Thus, the possibility exists that this conserved motif is targeted by both SOS2 and MPK6. If so, the putative phosphorylation of S1136 by MPK6 would prevent activation by SOS2 because the mutation S1136D abrogated SOS1 activity in planta (Fig. S2D). Like SOS1, the C terminus of the plasma membrane H⁺-ATPase includes an auto-inhibitory domain to inhibit the activity of the pump (21). PK5, a SnRK3 kinase similar to SOS2, phosphorylates the H⁺-ATPase isoform AHA2 at S931 in the C-terminal regulatory domain. Phosphorylation at this site inhibits interaction between the H⁺-ATPase and an activating 14–3–3 protein binding the neighboring phosphorylated residue T947, thereby preventing the activation of the pump (21). The motif RIDSPSK within the recognition site of SOS2 is also a putative 14–3–3-binding site, but it remains to be determined whether SOS1 interacts with 14–3–3 proteins. The

possible interplay between SOS2- and MPK6-dependent phosphorylation of SOS1 deserves future research.

Through the selection of hyperactive alleles of SOS1 we have identified critical residues for SOS1 activity. Class 1 mutations appeared to enhance both the basal activity (i.e., without SOS2–SOS3) and the SOS1 activity upon up-regulation by SOS2–SOS3. All these mutations affected either fully conserved amino acids or residues embedded in conserved motifs. Mutation E261K lies in a hydrophobic region predicted to be TM7 and affects a glutamic acid residue fully conserved among SOS1 proteins. Likewise, mutations A399V and A399T affect a fully conserved alanine residue in TM11. Mutation R551G affects an invariant arginine that is embedded in the conserved sequence DxRxRxLNGVQA-AYWxMLDEGRI (R551 underlined) in the cytosolic module shared by SOS1 and AtNHX8. In contrast, mutations S742L and V743I change residues that are not well conserved, although they lie in a short intervening sequence between two fully conserved P740 and P746 residues (sequence PLSVALP in *Arabidopsis*) at the boundary between the homologous regions of SOS1 and AtNHX8 and the C-terminal extension that is unique to SOS1 proteins. The significance of these amino acid substitutions for SOS1 activity or regulation is presently unclear. All but one class 2 mutation rendered C-terminally truncated SOS1 proteins with maximal activity that was independent of SOS2–SOS3, strongly indicating that the last 130 amino acids of SOS1 include an auto-inhibitory domain. By comparing the relative salt tolerance of yeast expressing serial truncations created downstream of K1005 (the most downstream class 2 mutation with full SOS1 activity) this inhibitory domain was mapped to the bipartite conserved sequences [K,R][D,E]HxGLxSWPE (amino acids 1005–1015) and Sx[R,K]Axx[L,I,V]S[L,M][F,Y]GS (amino acids 1033–1044) (Fig. S1B). Truncations downstream from these motifs produced SOS1 proteins locked in the basal state because they retained the auto-inhibitory domain but lacked the C-terminal phosphorylation site by SOS2 that acts to relieve SOS1 from auto-inhibition (Fig. S4B). On the other hand, mutations *sos1-8* (G777D) and *sos1-9* (G784E) created proteins that were still largely inactive even after removal of the auto-inhibitory domain (Fig. S4C). These two glycine residues are embedded in a very-well-conserved domain that shows weak similarity to a CNBD (Prosite pf00027). The null allele *sos1-7* creates a frameshift mutation starting in residue E759, thereby eliminating this domain and producing an inactive SOS1 protein in planta (14). Together, these data strongly suggest that this putative CNBD plays an important, yet undetermined, role in the activation of SOS1. Because a fragment comprising the auto-inhibitory domain interacted in the yeast system with SOS1Δ998 but not with SOS1Δ742, we suggest that the auto-inhibitory and the CNBDs interact to keep SOS1 inactive (Fig. S5). Upon salinity stress, the SOS2–SOS3 kinase complex phosphorylates the auto-inhibitory domain, thereby relieving SOS1 auto-inhibition. In this regard, it is worth noting that the class 2 mutation P985S lies in the intervening region between the CNBD and the auto-inhibitory domains. This mutation may remove a critical turn in the polypeptide secondary structure and disrupt the interaction between these two domains, thereby preventing SOS1 auto-inhibition.

Materials and Methods

Plasmid Constructs and Protein Production. GST-tagged fusion proteins used in phosphorylation assays and site-directed mutagenesis of serine 1136 and 1138 in SOS1 were produced according to standard methods, which are detailed in *SI Materials and Methods*, together with primer sequences in Table S2. For expression in *Arabidopsis*, SOS1 mutant alleles were subcloned in pBISOS1 (22) or pCAMBIA2300, both containing the 35S CaMV promoter.

Phosphorylation Assays. For in vitro assays with SOS2, different GST:SOS1 peptides were purified from yeast cells. Cells were collected by centrifugation and lysed with glass beads in PBS buffer (10 mM Na₂HPO₄, 2 mM KH₂PO₄,

2.7 mM KCl, 137 mM NaCl, pH 7.4) supplemented with 1% Triton X-100. SOS2T168D/Δ308 was expressed as a GST-tagged fusion protein in *E. coli* (17). Substrate recombinant proteins (~100 ng) were subjected to phosphorylation by the SOS2T168D/Δ308 protein kinase (~100 ng) in 30 μL of buffer (20 mM Tris-HCl, pH 7.5, 5 mM MgCl₂, 1 mM DTT). Reactions were started by adding ATP (0.2 mM with 1 μCi of [³²P]ATP), which was incubated at 30 °C for 30 min, and stopped with 10 μL of 4× SDS/PAGE sample buffer. Aliquots were then resolved by SDS/PAGE and the gel was exposed to X-ray films. To determine the phosphorylated residues, 20 μg of GST:SOS1998-1146 incubated with and without SOS2T168D/Δ308 were purified by 12% SDS/PAGE and subjected to nLC-MS/MS. For identification of protein modification, fragmentation spectra were searched against the Mass Spectrometry Protein Sequence DataBase using the Mascot software (Matrix Science). For SOS1 phosphorylation in planta, 2- to 3-wk-old plants were treated with 100 mM NaCl. Grinded leaves were extracted in 1 vol of extraction buffer (50 mM Tris-HCl, pH 7.5, 150 mM NaCl, 0.5% Nonidet P-40, 1 mM EDTA, 3 mM DTT, 2 mM Na₃VO₄, 2 mM NaF, 2 mM β-glycerophosphate) supplemented with a proteinase inhibitor mixture (1 mM phenylmethylsulfonyl fluoride, 5 μg/mL leupeptin, 1 μg/mL aprotinin, 1 μg/mL pepstatin, 5 μg/mL antipain, 5 μg/mL chymostatin, 50 μM MG132, 50 μM MG115, 50 μM μM ALLN). After separation in 6% SDS/PAGE, proteins were transferred to polyvinylidene difluoride membrane and detected with anti-HA (1:2,000) or anti-SOS1 (1:250) monoclonal antibodies. For phosphatase treatments, protein extracts were prepared either in λ-phosphatase buffer (50 mM Hepes, pH 7.5, 100 mM NaCl, 2.5 mM NaCl₂, 2 mM DTT, 0.01% Brij-35, 0.5% Triton X-100, 0.4% Nonidet P-40), or in calf intestinal phosphatase (CIP) buffer (50 mM Tris-HCl, pH 7.9, 100 mM NaCl, 10 mM MgCl₂, 1 mM DTT) supplemented with the proteinase inhibitor mixture described above. Fifty-microliter aliquots of protein extracts were incubated with 400 units of λ-protein phosphatase or with 10 units of CIP, with or without phosphatase inhibitors (2 mM NaF, 2 mM Na₃VO₄) at 30 °C for 5 min.

Ion Transport. The wild-type and SOS1G777D (*sos1-8*) proteins were His-tagged, purified from yeast plasma membrane by Ni²⁺ affinity chromatography, and reconstituted in artificial proteoliposomes as described (23). After imposing the internal acidification of vesicles, 50 mM Na₂S₂O₈ was added to the incubation buffer and Na/H exchange was monitored by changes in pyranine fluorescence (23). ATP (1.5 mM) was added to all samples and kinase SOS2T168D/Δ308 (1 μg) only when indicated.

Yeast Methods. *Saccharomyces cerevisiae* AXT3K strain (Δ*ena1::HIS3::ena4*, Δ*nha1::LEU2*, Δ*nhx1::KanMX4*) has been described elsewhere (24). Sodium tolerance tests were performed in the alkali cation-free medium AP (25) supplemented with 1 mM KCl and with NaCl as indicated for each experiment. For yeast two-hybrid, the SOS2 cDNA was amplified by PCR with oligos P14 and P15 and cloned in-frame between the NdeI and PstI sites of pAS2.1 (Clontech). The SOS1 fragments encompassing residues 441–997 and 998–1146 were amplified with the oligos P16 and P17 and P18 and P19, respectively, and cloned in-frame between the NcoI and BamHI sites of pACT2 (Clontech). All PCR products were sequenced. For the SRS, a 450-pb fragment extending from 2,993 bp downstream of the ATG to the end of the SOS1 ORF was amplified with primers P20 and P21 and inserted into plasmid pADNS to produce a translational fusion downstream from the hSos protein (19). The bait proteins were expressed from vector pYPGE15. All plasmids used for SRS were transformed in the *S. cerevisiae* strain *cdc25-2* (19).

Isolation of Hyperactive SOS1 Mutants. The plasmid pSOS1-1 (11), harboring the SOS1 cDNA, was transformed into the mutator strain Epicurian *E. coli* XL1-Red (Stratagene). Transformants were selected on LB plates containing ampicillin (100 μg/mL), pooled in six groups, and grown overnight at 37 °C in LB broth. Randomly mutated plasmid DNA extracted from individual pools was used to transform the yeast strain AXT3K. Mutations leading to increased salt tolerance were selected by plating transformants on AP medium containing 1 mM KCl and 150 mM NaCl. Plasmids were extracted from salt-resistant clones and rechecked in fresh transformants, and the SOS1 cDNA insert was fully sequenced to identify the mutations.

Antibody Production and Immunoblotting. Antibodies against SOS1 were produced according to modifications of standard techniques, detailed in *SI Materials and Methods*. Leaf extracts were immunoblotted following standard techniques.

ACKNOWLEDGMENTS. We are indebted to Unidad de Proteómica, Centro Nacional de Investigaciones Cardiovasculares Carlos III, for mass-spectrometric analysis. This work was supported by Grants BIO2009-08641 and CSD2007-

00057 from the Ministerio de Ciencia e Innovacion (cofinanced by Fondo Europeo de Desarrollo Regional) (to J.M.P. and F.J.Q.), World Class University

Program Grant R32-10148 (to D.-J.Y. and W.Y.K.), and National Institutes of Health Grants R01GM070795 and R01GM059138 (to J.-K.Z.).

1. Abrol IP, Yadav JSP, Massoud FI (1988) Salt-affected soils and their management. *FAO Soils Bull*, ed Food and Agriculture Organization (Rome).
2. Tester M, Davenport R (2003) Na⁺ tolerance and Na⁺ transport in higher plants. *Ann Bot* 91:503–527.
3. Munns R, Tester M (2008) Mechanisms of salinity tolerance. *Annu Rev Plant Biol* 59: 651–681.
4. Shi HZ, Quintero FJ, Pardo JM, Zhu JK (2002) The putative plasma membrane Na⁺/H⁺ antiporter SOS1 controls long-distance Na⁺ transport in plants. *Plant Cell* 14: 465–477.
5. Oh D-H, et al. (2009) Loss of halophytism by interference with SOS1 expression. *Plant Physiol* 151:210–222.
6. Olias R, et al. (2009) The plasma membrane Na⁺/H⁺ antiporter SOS1 is essential for salt tolerance in tomato and affects the partitioning of Na⁺ between plant organs. *Plant Cell Environ* 32:904–916.
7. Fraile-Escanciano A, Kamisugi Y, Cuming AC, Rodriguez-Navarro A, Benito B (2010) The SOS1 transporter of *Physcomitrella patens* mediates sodium efflux in planta. *New Phytol* 188:750–761.
8. Wu SJ, Ding L, Zhu JK (1996) SOS1, a genetic locus essential for salt tolerance and potassium acquisition. *Plant Cell* 8:617–627.
9. Zhu Z, Wu R (2008) Regeneration of transgenic rice plants using high salt for selection without the need for antibiotics or herbicides. *Plant Sci* 174:519–523.
10. Qi Z, Spalding EP (2004) Protection of plasma membrane K⁺ transport by the salt overly sensitive1 Na⁺-H⁺ antiporter during salinity stress. *Plant Physiol* 136:2548–2555.
11. Quintero FJ, Ohta M, Shi HZ, Zhu JK, Pardo JM (2002) Reconstitution in yeast of the Arabidopsis SOS signaling pathway for Na⁺ homeostasis. *Proc Natl Acad Sci USA* 99: 9061–9066.
12. Qiu QS, Guo Y, Dietrich MA, Schumaker KS, Zhu JK (2002) Regulation of SOS1, a plasma membrane Na⁺/H⁺ exchanger in Arabidopsis thaliana, by SOS2 and SOS3. *Proc Natl Acad Sci USA* 99:8436–8441.
13. Martínez-Atienza J, et al. (2007) Conservation of the salt overly sensitive pathway in rice. *Plant Physiol* 143:1001–1012.
14. Shi HZ, Ishitani M, Kim CS, Zhu JK (2000) The Arabidopsis thaliana salt tolerance gene SOS1 encodes a putative Na⁺/H⁺ antiporter. *Proc Natl Acad Sci USA* 97:6896–6901.
15. Mäser P, et al. (2001) Phylogenetic relationships within cation transporter families of Arabidopsis. *Plant Physiol* 126:1646–1667.
16. An R, et al. (2007) AtNHX8, a member of the monovalent cation: Proton antiporter-1 family in Arabidopsis thaliana, encodes a putative Li/H antiporter. *Plant J* 49:718–728.
17. Guo Y, et al. (2004) Transgenic evaluation of activated mutant alleles of SOS2 reveals a critical requirement for its kinase activity and C-terminal regulatory domain for salt tolerance in Arabidopsis thaliana. *Plant Cell* 16:435–449.
18. Gong DM, Guo Y, Jagendorf AT, Zhu JK (2002) Biochemical characterization of the Arabidopsis protein kinase SOS2 that functions in salt tolerance. *Plant Physiol* 130: 256–264.
19. Aronheim A (1997) Improved efficiency sos recruitment system: Expression of the mammalian GAP reduces isolation of Ras GTPase false positives. *Nucleic Acids Res* 25: 3373–3374.
20. Yu L, et al. (2010) Phosphatidic acid mediates salt stress response by regulation of MPK6 in Arabidopsis thaliana. *New Phytol* 188:762–773.
21. Fuglsang AT, et al. (2007) Arabidopsis protein kinase PKS5 inhibits the plasma membrane H⁺-ATPase by preventing interaction with 14-3-3 protein. *Plant Cell* 19: 1617–1634.
22. Shi HZ, Lee BH, Wu SJ, Zhu JK (2003) Overexpression of a plasma membrane Na⁺/H⁺ antiporter gene improves salt tolerance in Arabidopsis thaliana. *Nat Biotechnol* 21: 81–85.
23. Venema K, Quintero FJ, Pardo JM, Donaire JP (2002) The Arabidopsis Na⁺/H⁺ exchanger AtNHX1 catalyzes low affinity Na⁺ and K⁺ transport in reconstituted liposomes. *J Biol Chem* 277:2413–2418.
24. Quintero FJ, Blatt MR, Pardo JM (2000) Functional conservation between yeast and plant endosomal Na⁺/H⁺ antiporters. *FEBS Lett* 471:224–228.
25. Rodríguez-Navarro A, Ramos J (1984) Dual system for potassium transport in *Saccharomyces cerevisiae*. *J Bacteriol* 159:940–945.

Supporting Information

Quintero et al. 10.1073/pnas.1018921108

SI Materials and Methods

Site-Directed Mutagenesis and Recombinant Protein Production. A 2.1-kb BamHI fragment from the *SOS1* cDNA was subcloned into the BamHI site of the yeast expression vector pEG(KT) (1) to produce GST-tagged fusion proteins with the whole cytoplasmic region of *SOS1* (amino acids 441–1146; Fig. 2A). To generate GST-fused truncations of the C terminus of *SOS1* for phosphorylation assays, the following combinations were used: P1+P3 (*SOS1* residues 742–1146), P1+P4 (residues 742–997), and P2+P3 (residues 998–1146) (Table S2). All these fragments were subcloned in pEG(KT) with BamHI and XbaI. Site-directed mutagenesis of serine 1136 and 1138 in *SOS1* to alanine or aspartate was produced by PCR using the primer P5, which anneals just before a unique XhoI site in *SOS1*, and one of the following primers that introduce the corresponding mutation and a KpnI site downstream from the stop codon: P6 (S1136A), P7 (S1138A), or P8 (S1136A, S1138A). The corresponding PCR products were replaced in the wild-type *SOS1* cDNA in the yeast expression vector pSOS1-1 (2), sequenced to verify the presence of the mutation, and transformed in yeast. For the phosphorylation test, the whole cytosolic region (amino acids 441–1146) of *SOS1* mutants S1136A, S1138A, and S1136A/S1138A was fused to GST by amplification from the above-mentioned constructs with primers P9 and P3 and subcloned in pEG(KT). All recombinant proteins were affinity-purified on glutathione-Sepharose (GE Healthcare). For plant complementation, mutations in S1136 were created using primers P10 and P11 for S1136A and P12 with P13 for S1136D.

Arabidopsis Transformation and Complementation Test. Plasmid constructs were introduced into the *Agrobacterium* GV3101 (pMP90) strain and then transformed in the *Arabidopsis* mutant

sos1-1 by vacuum infiltration (3). Kanamycin-resistant T₂ transgenic plants were selected and subjected to complementation tests on Murashige and Skoog agar medium supplemented with NaCl, as indicated for each case. Culture was in an environmentally controlled chamber at 22 °C and a 16-h light/8-h dark cycle with photosynthetically active radiation of 30 μmol·m⁻²·s⁻¹.

Production of Monoclonal Antibodies Against *SOS1*. A fragment encoding the cytosolic domain of *SOS1* (amino acids 446–1146) fragment was amplified and cloned into pGEX-5x-3 to create a GST-translational fusion. The recombinant protein was purified by glutathione-Sepharose chromatography. Anti-*SOS1* antibodies were generated as described, with modifications (4). Antibody-producing B cells were generated by immunizing BALB/c mice four times with 50 μL GST:*SOS1* (20 μg) and an equal volume of adjuvant (Gerbu) for each immunization. The splenocytes of immunized mice were fused with follicular (FO) B cells, mouse myeloid line cells, using polyethylene glycol 1500 (Roche). Fused cells were resuspended in hybridoma-selection DMEM (Invitrogen) containing 20% FBS (Invitrogen) and hypoxanthine-aminopterin-thymidine (HAT) media supplement (Sigma). Cells were then plated in 96-well plates. After a 2-wk incubation, the hybridoma supernatants were tested using ELISA with GST:*SOS1*-coated (1 μg/well) ELISA plates (Nalgene). For purification of antibodies, hybridoma clones were intraperitoneally injected into 8-wk-old female BALB/c mice primed with 0.5 mL of incomplete Freund's adjuvant (Sigma) 1 wk previously. The ascetic fluids were collected after 1 wk. Supernatants were separated by centrifugation, and the antibodies in ascites were purified using protein-G agarose (KPL). Purity of antibodies was confirmed using Coomassie-blue staining in SDS/PAGE gels.

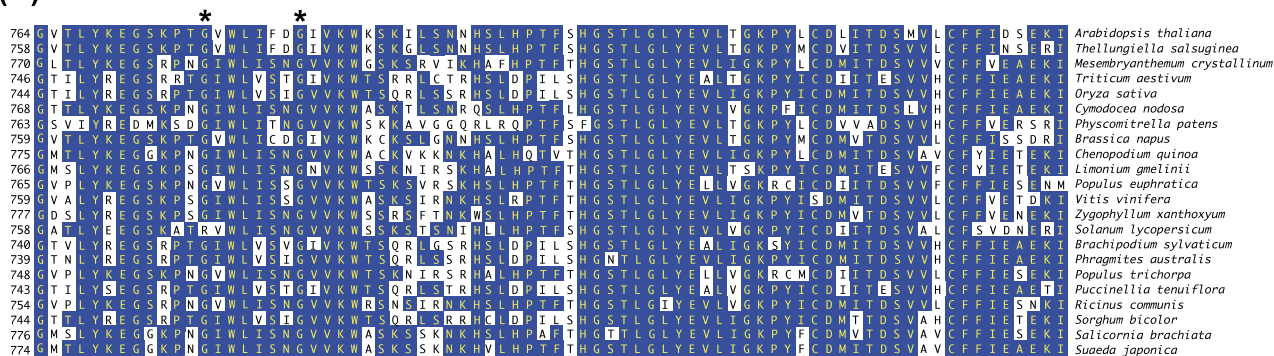
1. Pierce BD, Wendland B (2009) Sequence of the yeast protein expression plasmid pEG(KT). *Yeast* 26:349–353.

2. Quintero FJ, Ohta M, Shi HZ, Zhu JK, Pardo JM (2002) Reconstitution in yeast of the Arabidopsis SOS signaling pathway for Na⁺ homeostasis. *Proc Natl Acad Sci USA* 99: 9061–9066.

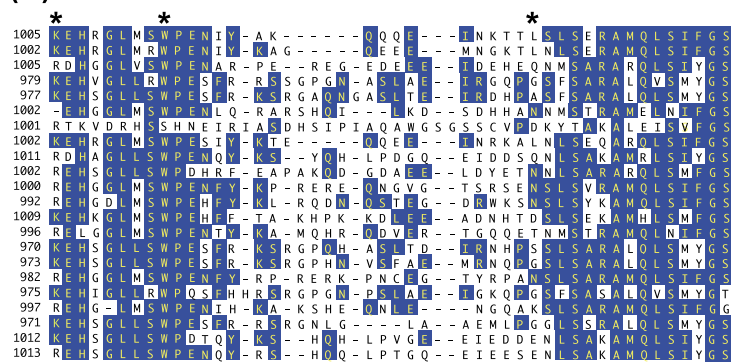
3. Clough SJ, Bent AF (1998) Floral dip: A simplified method for *Agrobacterium*-mediated transformation of *Arabidopsis thaliana*. *Plant J* 16:735–743.

4. Bae S, et al. (2010) Generation of anti-proteinase 3 monoclonal antibodies and development of immunological methods to detect endogenous proteinase 3. *Hybridoma (Larchmt)* 29:17–26.

(A)



(B)



(C)



Fig. S1. Sequence alignment of functional domains in SOS1 proteins. SOS1 sequences of the indicated species were aligned using CLUSTAL-W. Shown are the alignments corresponding to the putative cyclic nucleotide binding domain (A), the suggested auto-inhibitory domain (B), and the SOS2 phosphorylation site (C). The amino acid residues conserved in the majority of aligned proteins are highlighted. Relevant amino acids described in the text are indicated by asterisks. Underlining indicates the bipartite conserved sequence comprising the auto-inhibitory domain.

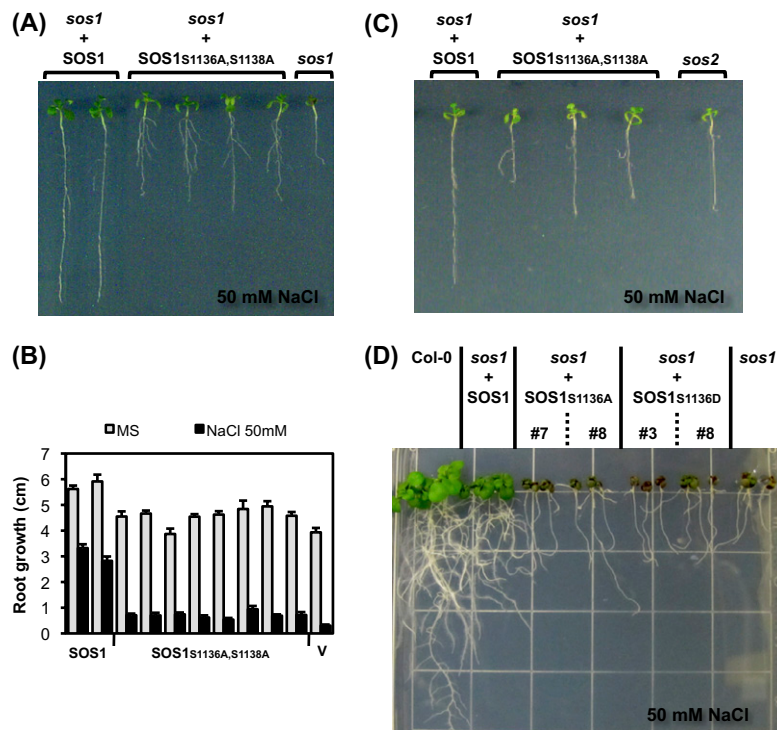


Fig. S2. Complementation test in planta with SOS1 mutant proteins. (A) The *Arabidopsis* mutant *sos1-1* was transformed to express a wild-type SOS1 protein or the mutant protein S1136A/S1138A, or with an empty vector. Eight independent lines (only four are depicted) expressing the S1136A/S1138A mutant protein were compared with two lines expressing the wild-type protein for growth in MS medium supplemented with 50 mM NaCl. (B) Root growth of the transgenic lines described in A after 15 d in Murashige–Skoog (MS) medium supplemented with 50 mM NaCl. (C) Transgenic *sos1-1* seedlings expressing wild-type and SOS1 mutant S1136A/S1138A proteins were compared with *sos2-2* seedlings in MS medium supplemented with 50 mM NaCl, as in B. (D) Four-day-old seedlings grown on MS agar medium were transferred to MS agar plates with or without 50 mM NaCl; photo was taken 14 d after transfer. The wild-type transgenic plants expressing SOS1, SOS1^{S1136A}, or SOS1^{S1136D} on *sos1-1* background and the *sos1-1* mutant plants are shown.

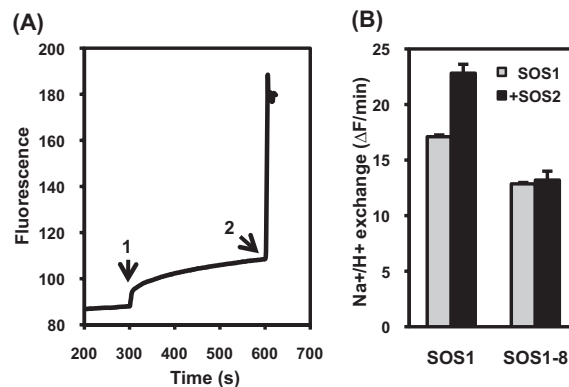


Fig. S3. Na/H exchange by SOS1 in proteoliposomes. (A) His-tagged proteins were purified and reconstituted in artificial proteoliposomes. Na/H exchange assays were measured using pyranine fluorescence to monitor proton fluxes. A typical trace is shown, where arrow 1 indicates addition of Na₂SO₄ (assay start, proton efflux) and arrow 2 indicates the addition of NH₄Cl (assay end, proton gradient dissipated). (B) Transport rates of wild-type SOS1 and mutant SOS1^{G777D} (*sos1-8* allele) with and without the addition of SOS2^{T168D/Δ308}. Shown are means and SE of three technical replicates. The experiment was repeated twice with independent protein preparations.

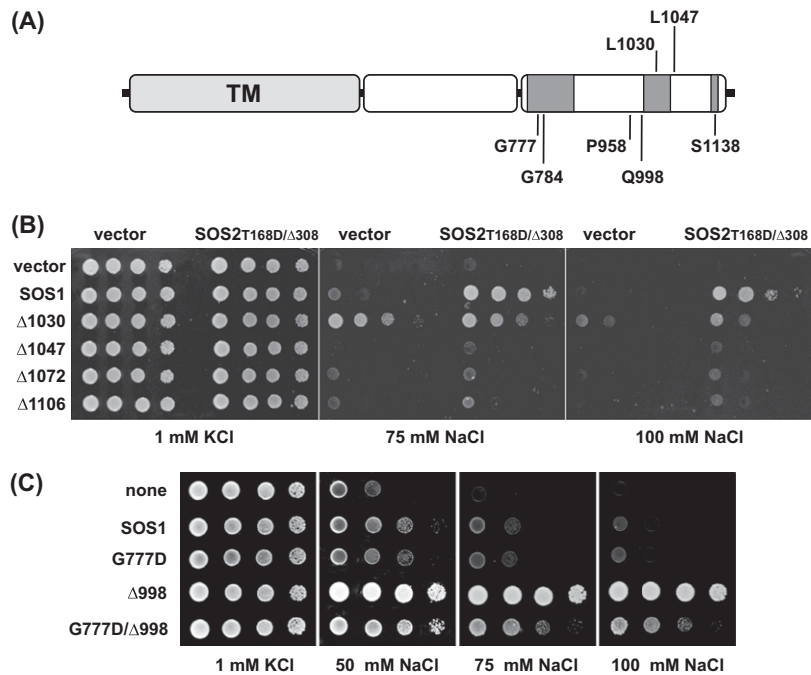


Fig. S4. Mapping the auto-inhibitory domain of SOS1. (A) Schematic of SOS1 depicting three domains: the N-terminal membranous domain (TM), the central domain that shares sequence homology to NHX8, and the C-terminal SOS1-specific domain. In the latter, three dark gray boxes represent the domain essential for SOS1 activity (*Left*), the auto-inhibitory domain (*Center*), and the SOS2 phosphorylation site (*Right*). Also shown are the positions of critical amino acid residues used to dissect the regulatory domains of SOS1. (B) SOS1 mutants bearing the indicated C-terminal truncations were transformed in strain AXT3K, with and without the coexpression of SOS2T168D/Δ308, and compared with wild-type SOS1 in AP medium (1 mM KCl) and the indicated concentrations of NaCl. Deletion of amino acid downstream residue 1030 relieved SOS1 from auto-inhibition in the absence of SOS2T168D/Δ308. (C) Negative dominance of mutation *sos1-8*. Mutation SOS1G777D (*sos1-8* allele) was combined with the removal of the auto-inhibitory domain of SOS1 (SOS1Δ998), and single- and double-mutant proteins were compared in AP medium (1 mM KCl) and the indicated concentrations of NaCl. Mutation G777D impeded the constitutive activation of SOS1 by removal of the C-terminal auto-inhibitory domain. Note that protein SOS1Δ998 supports the growth of AXT3K cells up to 800 mM NaCl (Fig. 4A).

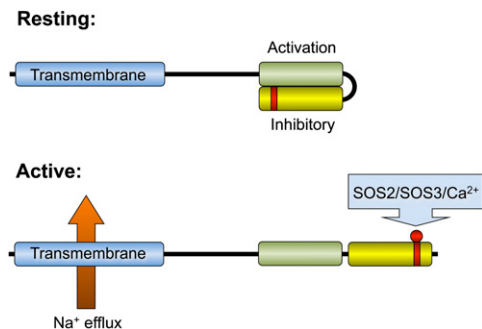


Fig. S5. Model representing the activation mechanism of SOS1. Without stress SOS1 is kept in a resting state because the C-terminal auto-inhibitory domain interacts with the adjacent activation domain that is essential for SOS1 activity. Upon salinity stress, the Ca^{2+} -dependent SOS2–SOS3 protein kinase complex phosphorylates SOS1 at serine 1138 (red circle) and relieves SOS1 from auto-inhibition, presumably by displacing the auto-inhibitory domain. Mutation of the proline 985 between the activation and auto-inhibitory domains may hinder their interaction, thereby resulting in a constitutively active full-length SOS1 protein.

Table S1. Hyperactive SOS1 mutants isolated in this study

Mutant class	Mutation	Position and protein change	No. of isolates
Class 1	E261K	Seventh transmembrane	1
	A399V, A339T	Eleventh transmembrane	2, 1
	R551G	Middle globular domain	1
	S742L	Beginning of SOS1-specific sequence	1
	V743I	Beginning of SOS1-specific sequence	1
Class 2	P985S	Beginning of auto-inhibitory domain	1
	Q998Z	Stop codon, truncation of last 148 aa	9
	Q1000Z	Stop codon, truncation of last 146 aa	16
	K1005-FS	Frame-shift, premature stop codon	2
	W1013Z	Stop codon, truncation of last 143 aa	9

